Chinese Chemical Letters 32 (2021) 3718–3732

Contents lists available at ScienceDirect

Chinese Chemical Letters

journal homepage: www.elsevier.com/locate/cclet

Review

Progress in mechanochromic luminescence of gold(I) complexes

Shiqi Cheng[a,1], Zhao Chen[b,1,*], Ya Yin[a,*], Yue Sun[a,*], Shenghua Liu[c,*]

[a] Hubei Key Laboratory of Catalysis and Materials Science, College of Chemistry and Material Sciences, South-Central University for Nationalities, Wuhan 430074, China
[b] Jiangxi Key Laboratory of Organic Chemistry, Jiangxi Science and Technology Normal University, Nanchang 330013, China
[c] Key Laboratory of Pesticide and Chemical Biology, Ministry of Education, College of Chemistry, Central China Normal University, Wuhan 430079, China

ARTICLE INFO

Article history:
Received 27 March 2021
Revised 23 May 2021
Accepted 24 May 2021
Available online 29 May 2021

Keywords:
Gold(I) complexes
Mechanochromic luminescence
Mechanisms
Molecular packings
Aurophilic interactions

ABSTRACT

Photophysical properties of organic and organometallic luminophors are closely related with their molecular packings, enabling the exploitation of stimuli-responsive functional luminescent molecules. Mechanochromic molecules, which can change their luminescence characteristics after mechanical stimulus, have received an increasing interest due to their promising applications in multifunctional sensors and molecular switches. During the past two decades, the development of gold(I) chemistry has been attracting the attention of plenty of researchers. Indeed, a variety of gold(I) complexes with fascinating photophysical behaviors have been discovered. This review focuses on the research progress in the different types of mechanoluminochromic gold(I) complexes, including mono-, bi- and multi-nuclear gold(I) systems. Their interesting luminescence behaviors of these gold(I)-containing luminogens upon mechanical stimulus and the proposed mechanisms of their observed mechanochromic luminescence are summarized systematacially. Moreover, this review will put forward an outlook about the possible opportunities and challenges in this significative scientific field.

1. Introduction

Organic and organometallic light-emitting materials are widely applied in many areas including optical devices, bioimaging and photoelectronic devices [1–12]. Especially, mechanochromic luminescence materials sensitive to external mechanical force have attracted considerable interest in both fundamental and applied research fields [13–19]. This type of stimulus-responsive smart materials can exhibit changes in emission color under mechanical stress. In general, mechanical force-responsive luminescence is expected to be triggered by chemical or physical change. Compared with chemical structural change, physical structural change is considered to be more advantageous for achieving reversible solid-state luminescence. It is well-known that the solid-state luminescence of luminophors relies strongly on their molecular packings and intermolecular interactions [20,21]. Therefore, different luminescence may be obtained from the same emissive molecule by adjusting the corresponding molecular stacking without involving the variation of chemical structure. Indeed, intermolecular non-covalent interactions, which contain halogen bonds, hydrogen bonds, C-H•••π stacking, π-π stacking, *etc.*, may be effectively manipulated *via* different types of external stimuli such as grinding, pressing, rubbing, or hydrostatic pressure, enabling the exploitation of highly-efficient mechanoluminochromic luminophors. Over the last two decades, a large number of mechanochromic luminophors have been discovered, and the majority of these reported mechano-responsive luminescent molecules are proved to be organic compounds. Meanwhile, a number of metal-organic complexes exhibiting mechanoluminochromic characteristics have also been reported.

Owing to the existence of attractive aurophilic interactions induced by the synergy of relativistic effects and dispersion forces, luminophors involving gold(I) complexes have aroused increasing attention [22–33]. To date, a series of gold(I) complexes possessing various photophysical properties have been reported. For example, in 2012, Luo *et al.* reported aggregation-induced emission (AIE)-active gold(I)-thiolate complexes [34]. Subsequently, in 2013, Liu *et al.* reported a gold(I) complex simultaneously exhibiting AIE and thermochromic luminescence properties [35]. Bright solid-state emission and mechanochromic luminescence with high contrast are two vital factors for high-performance mechanical force-responsive smart materials. Gold(I) complexes are expected to exhibit excellent AIE or strong aggregative-state luminescence fea-

* Corresponding authors.
E-mail addresses: chenzhao666@126.com (Z. Chen), zyzyyy@outlook.com (Y. Yin), suny@scuec.edu.cn (Y. Sun), chshliu@mail.ccnu.edu.cn (S. Liu).
[1] These authors contributed equally to this work.

https://doi.org/10.1016/j.cclet.2021.05.049
1001-8417/

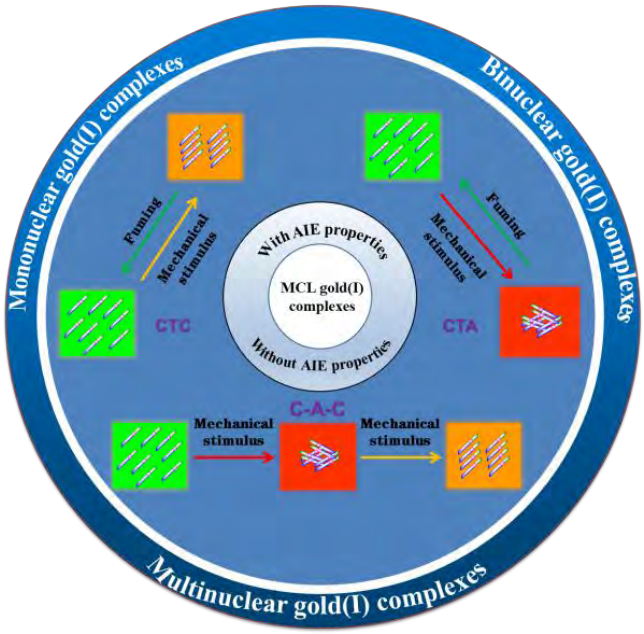

Scheme 1. Mechanochromic luminescence of gold(I) complexes.

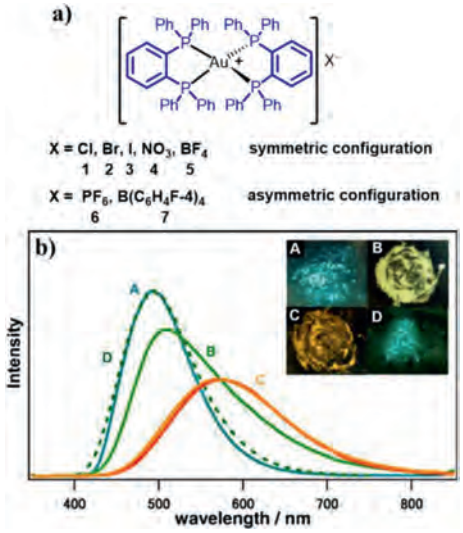

Fig. 1. (a) Molecular structures of complexes **1–7**. (b) Corrected emission spectra ($\lambda_{exc} = 350$ nm) and the insets show photographic images of **5** in various states under UV irradiation. Reproduced with permission [37]. Copyright 2010, Wiley-VCH (For interpretation of the references to color in this figure, the reader is referred to the web version of this article.).

ture triggered by intriguing aurophilic Au•••Au interactions, which is beneficial for the preparation of high-efficiency mechanochromic luminophors. In addition, given the fact that intramolecular and intermolecular aurophilic Au•••Au interactions may be controlled by the method of external mechanical stress [36], introducing gold(I)-containing structural units into suitable molecule skeletons is a rational strategy for the development of mechanoluminochromic metal complexes. Motivated by the effective design idea, a variety of mechanochromic luminescent gold(I) complexes with various auxiliary ligands have been synthesized. Although the corresponding examples about the detailed applications of these gold(I) complexes are still rather rare, it is no doubt that these mechanically responsive luminescence gold(I) complexes are promising candidates for the development of mechanical sensors and molecular switches. To date, there is no relevant review summarizing AIE and non-AIE-active mechanochromic luminescence gold(I) complexes in the last two decades. Indeed, it is significative for the development of stimuli-responsive gold(I) chemistry to summarize and discuss the researches related to AIE and non-AIE-active gold(I)-bearing luminophors with mechanochromism.

In this review, we will provide a comprehensive summary of progress in mechanoluminochromic gold(I) complexes (Scheme 1). More specifically, the review can be divided into three sections according to the number of Au(I) units in the molecular structures. The mechanochromic luminescence of reported AIE and non-AIE-active gold(I) complexes including mononuclear, binuclear, and multinuclear gold(I) units will be summarized. Meanwhile, their mechanochromic mechanisms of these gold(I) complexes will be also discussed. Finally, this review is expected to provide a valuable reference for designing high-efficient mechanochromic gold(I)-containing luminophors.

2. Mononuclear Au(I) complexes with mechanochromic luminescent (MCL) characteristics

With the rapid development of mechano-responsive gold(I) complexes, many mononuclear MCL gold(I) complexes with AIE or non-AIE effect have been reported. For AIE-active mononuclear MCL gold(I) complexes, crystalline-to-amorphous (CTA) phase transition is responsible for their observed MCL phenomena, while as for non-AIE-active mononuclear gold(I) complexes, their MCL phenomena are attributed to CTA phase transition, crystalline-to-crystalline (CTC) phase transition or uncertain mechanisms.

2.1. Mononuclear MCL Au(I) complexes without AIE effect

2.1.1. The MCL phenomena resulting from CTA phase transition

Osawa *et al.* designed a series of tetrahedral Au(I) complexes **1–7** to study the effect of counter anions on their mechanochromic behaviors (Fig. 1a) [37]. Indeed, the types of counter anions could directly affect their mechanochromic properties. Compared with complexes **6** and **7**, complexes **1–5** possessed smaller counter anions, and these complexes showed intense blue phosphorescence. Complexes **1–7** exhibited obvious MCL behaviors. For example, as shown in Fig. 1b, the strong blue phosphorescence of microcrystalline sample of **5** was finally converted to yellow-orange luminescence with a yellow-emitting intermediate state after continuous grinding for an hour. Upon treating the yellow-orange-emitting sample with diethyl ether, the initial blue luminescence was observed again. The powder X-ray diffraction (PXRD) measurements of **5** in various solid states demonstrated that its MCL phenomenon was attributed to the morphological interconersion between the crystalline and amorphous states. Similarly, complexes **1**, **2**, **3**, **6** and **7** also displayed MCL responses resulting from CTA phase transition. Notably, for MCL complex **4**, "a mechanical equilibrium" of crystalline and amorphous states could be achieved after consecutive grinding.

Baranyai *et al.* reported a mononuclear gold(I)-diphosphine complex [38]. Interestingly, the complex displayed both mechanochromic and MCL characteristics. Upon mechanical grinding, complex **8** changed its color from white to yellow. Meanwhile, its blue luminescence was transformed into the red luminescence (Fig. 2). By analyzing the obtained PXRD results, the authors discovered that the crystallinity of **8** gradually decreased with the increasing of grinding time, and an amorphous state was obtained after 13 min of ball-milling. Furthermore, the original crystalline state was restored upon treating with methanol solvent. Therefore, the reversible mechanochromic and MCL behaviors could be attributed to the CTA and amorphous-to-crystalline phase transitions.

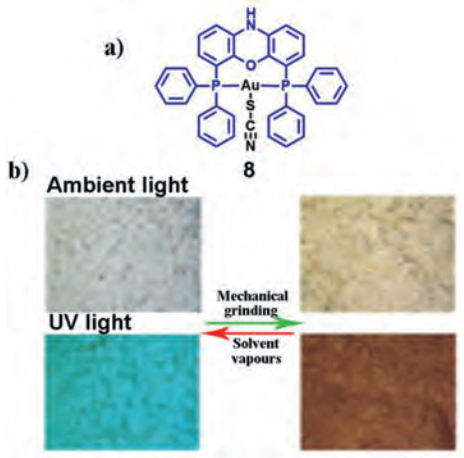

Fig. 2. (a) The molecular structure of complex **8**. (b) Photographs of complex **8** in different states (before grinding, after grinding, and after treating with dichloromethane) under ambient light and 365 nm UV light. Reproduced with permission [38]. Copyright 2015, The Royal Society of Chemistry (For interpretation of the references to color in this figure, the reader is referred to the web version of this article.).

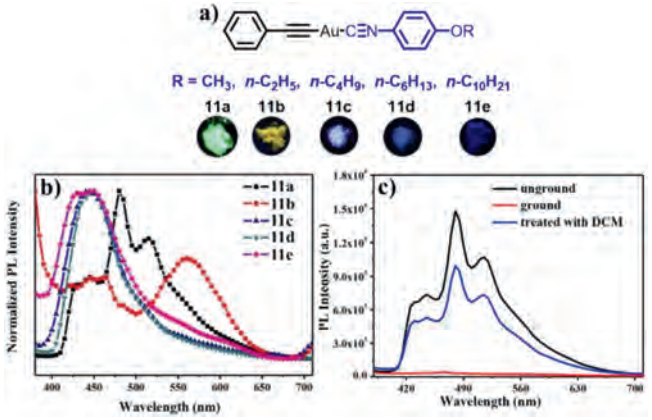

Fig. 4. (a) Molecular structures of complexes **11a–11e** and photographic images of solid samples **11a–11e** under 365 nm UV light. (b) Photoluminescence spectra of **11a–11e** in the solid state, excitation wavelength: 365 nm. (c) Photoluminescence spectra of **11a** in various solid states, excitation wavelength: 365 nm. Reproduced with permission [41]. Copyright 2018, Elsevier Ltd. (For interpretation of the references to color in this figure, the reader is referred to the web version of this article.).

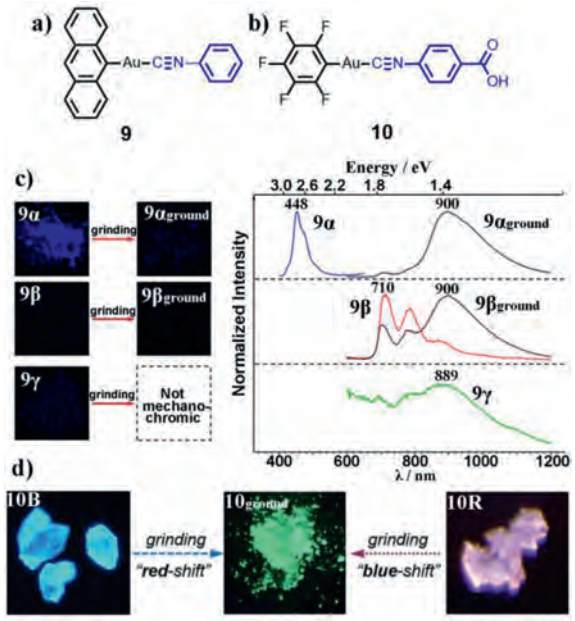

Fig. 3. Molecular structures of complexes **9** (a) and **10** (b). (c) Photoluminescence photographs and emission spectra of **9α**/**9β**/**9γ** before and after grinding, excitation wavelength: 365 nm. Reproduced with permission [39]. Copyright 2017. American Chemical Society. (d) Photoluminescence photographs of **10B** and **10R** before and after grinding, excitation wavelength: 365 nm. Reproduced with permission [40]. Copyright 2018, The Royal Society of Chemistry (For interpretation of the references to color in this figure, the reader is referred to the web version of this article.).

Seki *et al.* described a mononuclear gold(I) isocyanide complex **9** with an anthryl unit (Fig. 3a) [39]. Excitingly, the authors obtained three polymorphs **9*α***, **9*β*** and **9*γ*** with different luminescence properties of **9**. For polymorphs **9*α*** and **9*β***, the emission maxima were bathochromically shifted to 900 nm in response to mechanical grinding, exhibiting mechano-responsive IR-emissive feature (Fig. 3c). Moreover, polymorph **9*γ*** with IR-emissive behavior was also obtained, which was beneficial to the deep understanding of the rare mechanochromic IR emission. In 2018, Seki *et al.* synthesized an arylgold (arylisocyanide) complex **10**, and recrystallization of complex **10** from dichloromethane/methanol provided two polymorphs **10B** and **10R** [40]. Interestingly, polymorph **10B** exhibited MCL behavior with bathochromic spectral shift, while polymorph **10R** exhibited MCL behavior with hypsochromic spectral shift (Fig. 3d). It was speculated that the variations of their intermolecular aurophilic interactions were opposite after grinding **10B** and **10R**. For **10B**, intermolecular aurophilic interactions were formed upon grinding, which resulted in red-shifted luminescence. While for **10R**, intermolecular aurophilic interactions became weaker upon grinding, which caused blue-shifted luminescence.

Dong *et al.* reported five mononuclear gold(I) isocyanide complexes **11a–11e** with alkyl chains of different lengths [41]. The solid-state emission behaviors of these complexes could be affected by the alkyl chain length. Indeed, **11a–11e** displayed various solid-state luminescence (Fig. 4a), and these complexes showed different luminescent spectra in the solid state (Fig. 4b). Furthermore, upon grinding, **11a–11e** all exhibited mechanochromic luminescence quenching properties. Taking complex **11a** as a representative example, as shown in Fig. 4c, after grinding, the green emission band with the maximal emission peak at 480 nm almost disappeared, indicating that **11a** possessed a force-induced emission quenching feature. The formation of strong intermolecular interactions and conformation planarization after grinding were responsible for luminescence quenching phenomena. On the other hand, the PXRD results demonstrated that the mechanical force-responsive luminescence quenching processes of **11a–11e** involved the CTA morphological transition.

Chen, Liu and coworkers designed and synthesized a series of triphenylamine, carbazole or tetraphenylethylene-based MCL mononuclear gold(I) complexes. For example, the as-synthesized complexes **12a** and **12b** displayed reversible bathochromic or hypsochromic MCL behavior respectively, whereas the pristine complex **12c** displayed irreversible hypsochromic MCL phenomenon [42]. For complex **13**, it showed self-reversible MCL phenomenon involving color change from yellow to yellow-green [43]. As for complexes **14–16**, they exhibited contrasting mechano-responsive emissive behaviors [44]. More specifically, **14** showed luminescence on-off MCL phenomenon with yellow luminescence disappeared after grinding (Fig. 5). **15** also showed switchable MCL phenomenon between yellow–green and colorless. In contrast, no MCL phenomenon was observed for **16**. The noticed mechanical force-responsive characteristics of **12–15** were ascribed to CTA phase transition.

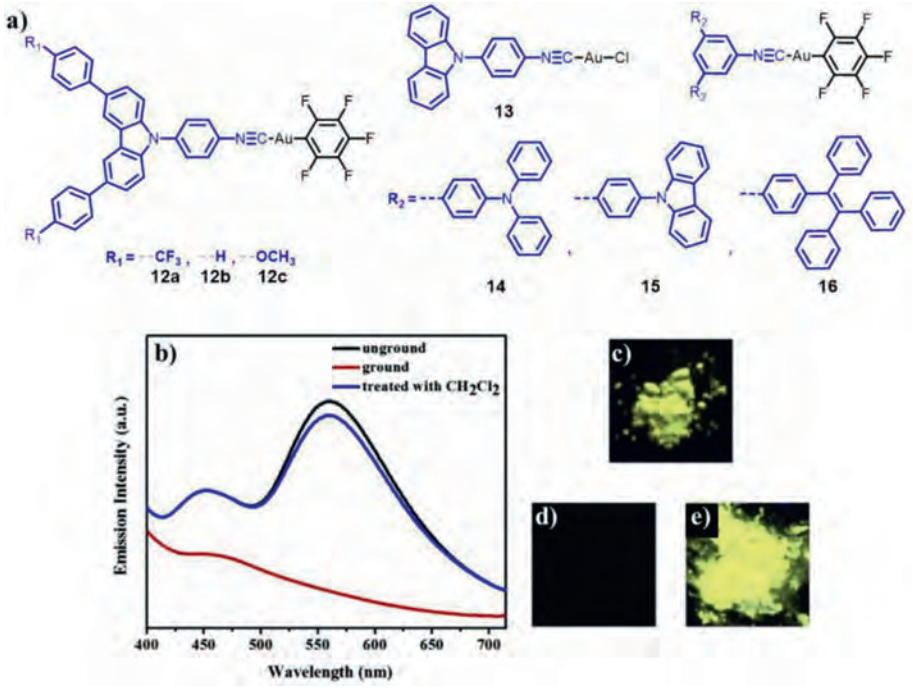

Fig. 5. (a) Molecular structures of complexes **12–16**. (b) PL spectra of complex **14** in various solid states, excitation wavelength: 365 nm. Photographic images of complex **14** in various solid states under 365 nm UV light: (c) the unground sample, (d) the ground sample, (e) the sample after treatment with dichloromethane. Reproduced with permission [44], Copyright 2018. Elsevier Ltd. (For interpretation of the references to color in this figure, the reader is referred to the web version of this article.).

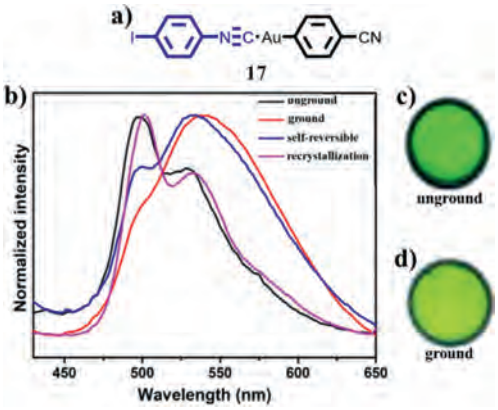

Fig. 6. (a) Molecular structure of complex **17**. (b) Solid-state emission spectra of complex **17** in various states. (c) Photoluminescence image of unground complex **17** under 365 nm UV irradiation. (d) Photoluminescence image of ground complex **17** under 365 nm UV irradiation. Reproduced with permission [45]. Copyright 2019, American Chemical Society (For interpretation of the references to color in this figure, the reader is referred to the web version of this article.).

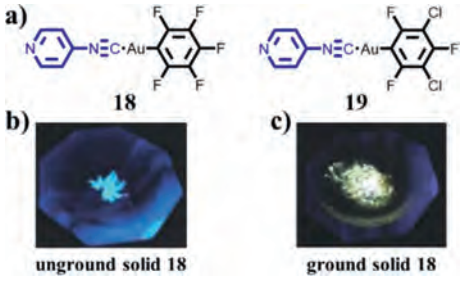

Fig. 7. (a) Molecular structures of complexes **18** and **19**. (b) Photoluminescence image of unground complex **18** under 365 nm UV irradiation. (c) Photoluminescence image of ground complex **18** under 365 nm UV irradiation. Reproduced with permission [46]. Copyright 2019, The Royal Society of Chemistry (For interpretation of the references to color in this figure, the reader is referred to the web version of this article.).

Wang *et al.* synthesized an aryl gold(I) isocyanide complex **17** [45]. As can be seen in Fig. 6, after heavy grinding, green light-emitting solid of **17** was changed into yellow light-emitting solid with the CTA transformation process, and the recrystallization of ground solid **17** could restore its initial green luminescence. Interestingly, the crystalline phase was also recovered when ground solid **17** was placed at room temperature for 10 h, and thus complex **17** showed an unusual self-reversible MCL feature. It was speculated that the mechanically triggered amorphous state could be restored to the initial crystalline state over a lower energy barrier at room temperature *via* an effective synergistic action of weak intermolecular halogen bonds and $\pi\cdots\pi$ stacking interactions.

Espinet *et al.* reported two MCL gold(I) isocyanide complexes **18** and **19** [46]. Upon grinding, the blue luminescence of solid **18** changed to a bright yellow luminescence (Fig. 7), and the green luminescent solid **19** was also converted to the similar yellow light-emitting solid. PXRD measurements demonstrated that blue light-emitting sample **18** and green light-emitting sample **19** lost crystalline nature after grinding. It was possible that different molecular packings of unground solids **18** and **19** were transformed into almost identical molecular stackings accompanied by shorter Au•••Au distances upon grinding, which were responsible for the observed mechanically induced red-shifted luminescence of complexes **18** and **19**.

2.1.2. The MCL phenomena resulting from CTC phase transition

CTC transformation caused by a mechanical stimulus is a very significative phenomenon, and it provides a molecular-level understanding of mechanochromic process. The single-crystal-to-single-crystal (SCSC) transformation of a gold(I) isocyanide complex **20** (Fig. 8) was firstly observed by Ito *et al.* in 2013 [47]. The authors obtained two polymorphs **20b** and **20y**, which emitted blue luminescence and yellow luminescence respectively, by means of rapid

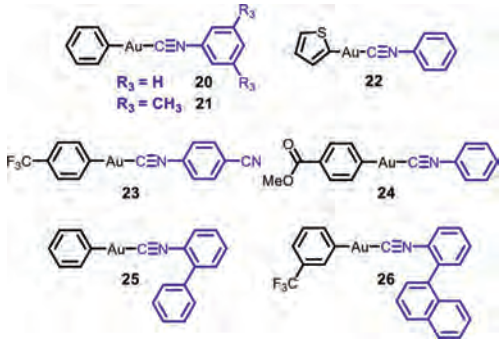

Fig. 8. Molecular structures of complexes **20–26**.

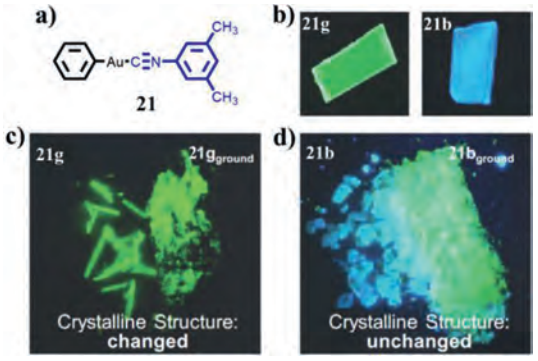

Fig. 9. (a) Molecular structure of complex **21**. (b) Photoluminescence images of polymorphs **21g** and **21b**. (c) Photoluminescence images of unground **21g** and ground **21g**. (d) Photoluminescence images of unground **21b** and ground **21b**. Reproduced with permission [49]. Copyright 2015, The Royal Society of Chemistry (For interpretation of the references to color in this figure, the reader is referred to the web version of this article.).

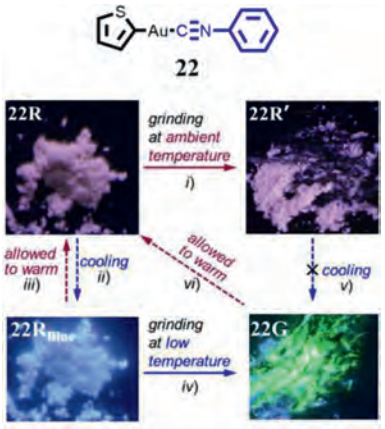

Fig. 10. Molecular structure of complex **22**, and schematic diagram of low-temperature-selective mechanochromic behavior of **22**. Reproduced with permission [50]. Copyright 2017, The Royal Society of Chemistry.

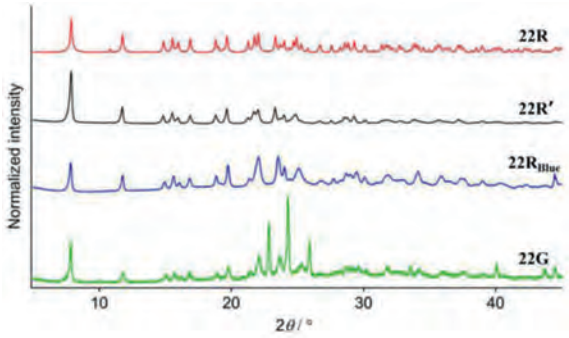

Fig. 11. PXRD patterns of **22R**, **22R'**, $\mathbf{22R_{Blue}}$ and **22G**. Reproduced with permission [50]. Copyright 2017, The Royal Society of Chemistry (For interpretation of the references to color in this figure legend, the reader is referred to the web version of this article.).

crystallization or slow crystallization from hexane/CH_2Cl_2. Interestingly, for polymorph **20b**, upon mechanical stimulus, the emission color was changed from blue to yellow with a SCSC molecular domino transformation, and the molecular packing of the resulting yellow light-emitting crystal was similar to that of polymorph **20y**. The observed SCSC transformation involving a conversion from C-H•••π to intermolecular gold-gold interactions was characterized by single crystal X-ray analysis. The phase transition was accompanied by an obvious emission color change, which allowed a clear visualization of phase transition.

Similarly, Ito *et al.* synthesized the methyl-substituted analogue of complex 20 [48], which formed polymorph **21g** with green emission and polymorph **21b** with blue emission. Notably, the whole single crystal **21g** could be converted to a blue-emitting single crystal **21b** *via* a weak mechanical stimulation-induced SCSC phase transition. Furthermore, as shown in Fig. 9, for **21g**, it showed no change of luminescent color after heavy grinding [49]. However, a prominent crystalline structural change was noticed. Conversely, **21b** exhibited an obvious change of luminescent color, but it retained its initial crystalline structure upon strong grinding [49].

In 2017, Ito *et al.* prepared a thienyl gold(I) isocyanide complex **22** exhibiting low-temperature-selective mechanochromic behavior [50]. The complex did not display MCL phenomenon at room temperature. In contrast, when cooled below −50 °C, complex **22** showed notable MCL phenomenon (Fig. 10). As exhibited in Fig. 11, PXRD patterns indicated that the luminescent transformation from blue light-emitting $\mathbf{22R_{Blue}}$ to green light-emitting **22G** upon grinding below −50 °C was attributed to crystalline structure changes.

Ito *et al.* reported a systematic screening approach to discover mechanochromic compounds exhibiting a CTC phase transition [51]. The authors synthesized **48** *para*-substituted (R^4) phenyl[*para*-substituted (R^5) phenyl isocyanide]gold(I) complexes (Fig. 12). An effective three-step screening program was then performed. Consequently, two gold(I) complexes **20** and **23** showed a CTC phase transition after mechanical stimulation. For complex **23**, the PXRD pattern of its ground sample also displayed many intense diffraction peaks, which were different from those in the PXRD pattern of its unground sample. This implied that complex **23** undergone a CTC phase transition upon applying mechanical stimulation.

Ito *et al.* prepared a mononuclear gold(I) complex **24** [52]. Upon ball milling of its crystals **24B** with blue luminescence, a CTC phase transition occurred, and a yellow-emitting powder $\mathbf{24Y_G}$ was obtained. Notably, both the luminescent characteristics and morphological structure of $\mathbf{24Y_G}$ were similar to those of crystals **24Y** obtained upon photoirradiation of **24B**. This is the first report of mechanical force promoting a phase transition to a photo-accessible crystalline phase.

In 2017, Ito *et al.* reported a gold(I) complex **25** containing a biphenyl unit, which afforded two types of crystals that involved chiral crystal **25ch** and achiral crystal **25ac** (Fig. 13) [53]. Upon grinding, the chiral crystal **25ch** was converted into achiral crystal $\mathbf{25g_{round}}$, which possessed a crystal structure similar to **25ac**. It is the first example of mechanical-stimulation-triggered chiral-crystal-to-achiral-crystal phase transition with a clear luminescence change. Subsequently, in 2018, Ito *et al.* reported a MCL gold(I) isocyanide complex **26** with a mechanical-cutting-triggered

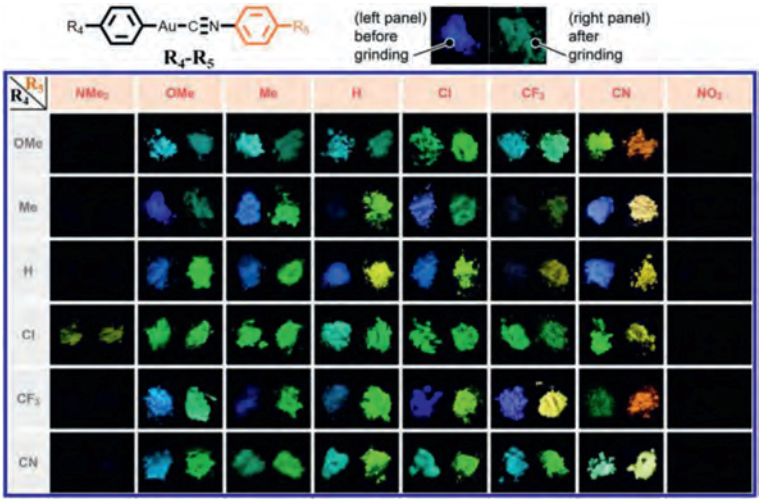

Fig. 12. Photographs of the **48** gold(I) complexes before and after grinding under 365 nm UV light. Reproduced with permission [51]. Copyright 2016, American Chemical Society.

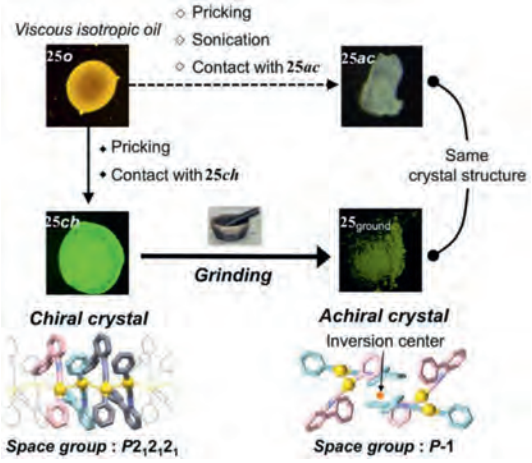

Fig. 13. Photographs of **25o**, **25ch**, **25g$_{round}$**, and 25ac recorded under UV irradiation, and the schematic diagram of phase transitions. Reproduced with permission [53]. Copyright 2017, American Chemical Society.

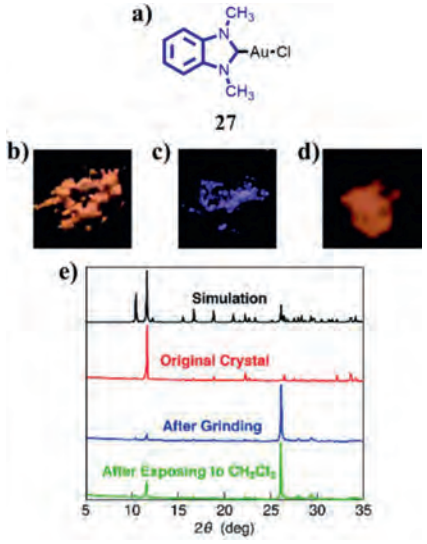

Fig. 14. (a) Molecular structure of complex **27**. Photoluminescence images of complex **27** in various states under 365 nm UV light: (b) unground, (c) ground, (d) vapor-exposure. (e) PXRD patterns of simulation based on single crystal **27** and single crystal **27** in various states. Reproduced with permission [55]. Copyright 2018, Springer (For interpretation of the references to color in this figure, the reader is referred to the web version of this article.).

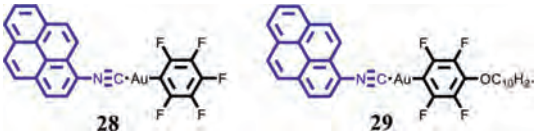

Fig. 15. Molecular structures of complexes **28** and **29**.

SCSC phase transition feature [54]. More interestingly, the complex firstly achieved the reverse phase transition of the obtained crystalline phase after mechanical stimulus *via* the method of vapor-induced SCSC phase transition.

In 2018, Hisano *et al.* reported a MCL gold(I) *N*-heterocyclic carbene complex **27** (Fig. 14a) [55]. Aurophilic interactions were considered to be the key factor for the observed MCL behavior of **27**. As can be seen in Fig. 14b, the initial crystals **27** obtained by recrystallization emitted orange luminescence due to the presence of intermolecular gold-gold interactions. Upon grinding, the gold-gold interactions were destroyed and the orange luminescence changed into the blue luminescence (Fig. 14c). According to the PXRD pattern of ground crystals **27** (Fig. 14e), some sharp diffraction peaks were noticed, which implied that the ground crystals **27** was also crystalline phase state. The orange luminescence could be restored completely in the presence of dichloromethane vapor (Fig. 14d). However, the corresponding PXRD pattern recovered only partially (Fig. 14e), which was due to the possibility that morphological structure recovered only occurred in the surface of the crystal.

Liu *et al.* prepared two pyrene-based gold(I) complexes **28** and **29** (Fig. 15) [56]. **28** and **29** exhibited similar reversible MCL phenomena between blue and green emissions, and the green luminescence came from mechano-triggered excimer emission, which was induced by the amorphization of crystalline samples **28** and **29**. Furthermore, the MCL behavior of **29** was self-reversible.

2.1.3. The mcl phenomena resulting from uncertain mechanisms

Laguna *et al.* reported a gold(I)-containing heterodimetallic complex $\{Tl[Au(C_6Cl_5)_2]\}_n$ (**30**, Fig. 16) [57]. After gentle crushing, the emission maximum of its crystals exhibited a blue shift from 560 nm to 547 nm at 77 K. Deák *et al.* prepared a heterodimetallic coordination polymer $Me_3Sn[Au(CN)_2]$ (**31**, Fig. 16) [58], and

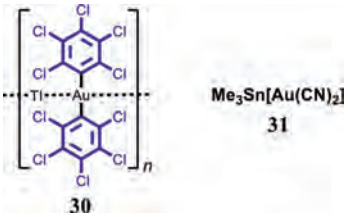

Fig. 16. Molecular structures of complexes **30** and **31**.

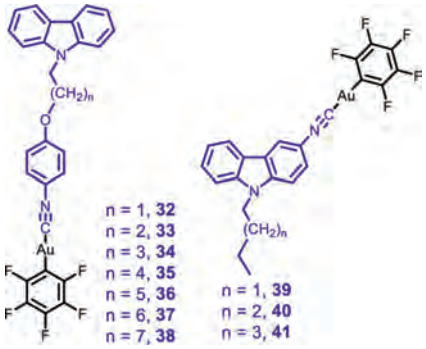

Fig. 17. Molecular structures of complexes **32–41**.

its pink emission was converted into the blue luminescence upon grinding. However, the MCL mechanisms of **30** and **31** are still unknown.

2.2. Mononuclear AIE-active MCL Au(I) complexes

Chen *et al.* synthesized seven carbazole-containing gold(I) isocyanide complexes **32–38** (Fig. 17), and these complexes possessed alkyl chains of different lengths [59]. All these obtained gold(I) complexes displayed typical AIE and reversible MCL characteristics. The MCL mechanism of **32–38** was ascribed to CTA phase transition. Meanwhile, the observed AIE and MCL phenomena were associated with the formation or alteration of intermolecular C-H•••F, π•••π, and aurophilic interactions.

In 2016, Chen *et al.* reported three mononuclear gold(I) complexes **39–41** (Fig. 17) [60]. These complexes showed excellent AIE feature involving luminescent color transformation from colorless to green upon aggregation. Furthermore, **39–41** also showed reversible MCL behaviors. For example, the yellow-green luminescence of the as-prepared complex **40** was converted into the green luminescence after grinding, and the original yellow-green luminescence could be restored completely when the ground powder of **40** was fumigated with dichloromethane vapor for 1 min (Fig. 18).

Chen *et al.* synthesized three AIE-active fluorene-based mononuclear gold(I) isocyanide complexes **42–44** (Fig. 19) [61], and complex **42** without containing alkyl chains exhibited reversible MCL phenomenon involving interconversion between green and faint yellow luminescence, and its MCL behavior was resulted from CTA phase transition. In contrast, complexes **43** and **44** with various alkyl chains did not show any MCL effect.

In 2017, Chen *et al.* reported a carbazole-based AIE-active gold(I) isocyanide complex **45** [62], and this complex could emit long-lived room-temperature phosphorescence with a luminescence lifetime up to 86.84 ms in the solid state. Upon grinding, its bright yellow phosphorescence was changed into yellow-green luminescence, and thus exhibiting MCL behavior (Fig. 20). In addition, **45** also showed vapochromic luminescence behavior. It is the first report of an AIE-active gold(I) complex possessing persistent room-temperature phosphorescence and multistimuli-responsive properties.

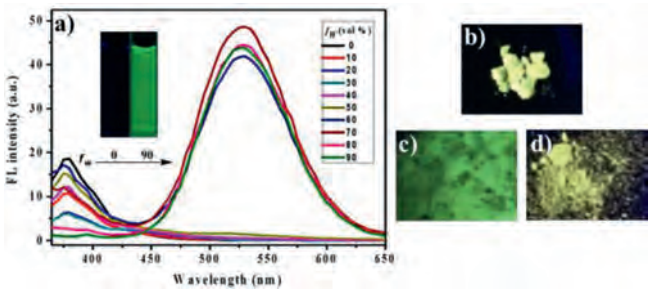

Fig. 18. (a) Emission spectra of complex **40** (2.0×10^{-5} mol/L) in DMF-H_2O mixtures with different water contents (0–90%), excitation wavelength: 350 nm. Photographic images of complex **40** in various solid states under 365 nm UV light: (b) the unground sample, (c) the ground sample, (d) the sample after treatment with dichloromethane. Reproduced with permission [60]. Copyright 2016, Elsevier Ltd. (For interpretation of the references to color in this figure, the reader is referred to the web version of this article.).

Fig. 19. Molecular structures of complexes **40–44**.

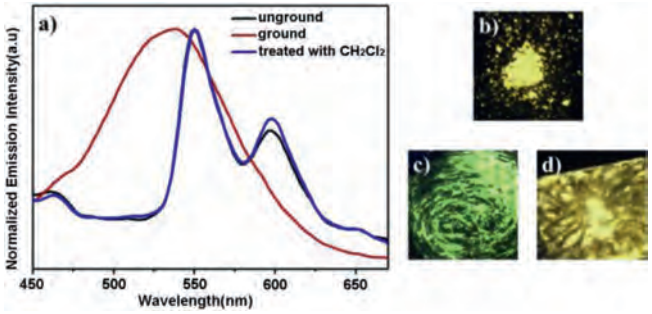

Fig. 20. (a) Solid-state emission spectra of complex **45** in various solid states, excitation wavelength: 365 nm. Photographic images of complex **45** in various solid states under 365 nm UV light: (b) the unground sample, (c) the ground sample, (d) the sample after treatment with dichloromethane. Reproduced with permission [62]. Copyright 2017, Elsevier Ltd. (For interpretation of the references to color in this figure, the reader is referred to the web version of this article.).

Yuan *et al.* reported a tetraphenylethene-containing mononuclear gold(I) complex **46**, which exhibited aggregation induced phosphorescence nature [63]. Owing to the synergistic effects of conformation planarization and the formation of intermolecular aurophilic interactions, the phosphorescent color of solid sample **46** changed from blue to green after grinding, and this observed MCL phenomenon was associated with CTA phase transition.

3. Mechanochromic luminescence of binuclear gold(I) complexes

To date, many binuclear gold(I) complexes have been found to be able to show MCL behavior. Consistent with the source of mechanochromic luminescence of mononuclear gold(I) complexes, the MCL mechanism of a majority of binuclear gold(I) complexes is

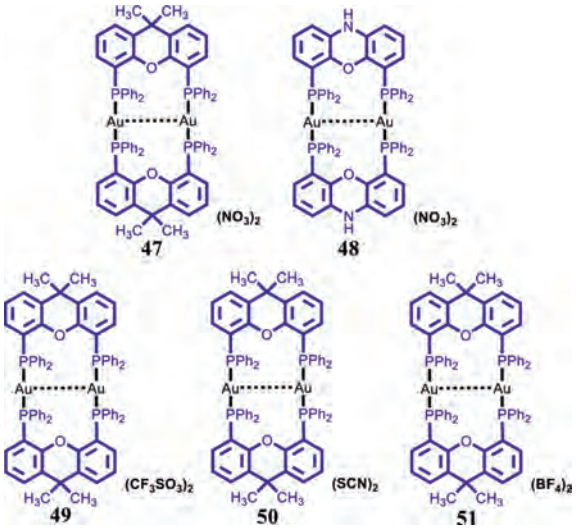

Fig. 21. Molecular structures of complexes **47–51**.

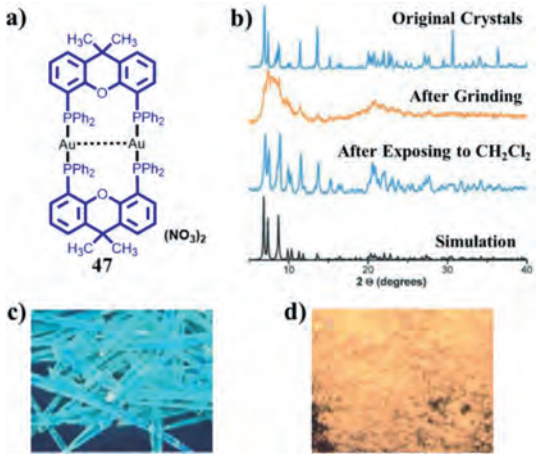

Fig. 22. (a) Molecular structure of complex **47**. (b) PXRD patterns of crystals **47** in various states and simulation based on single crystal **47**. Photoluminescence images of blue light-emitting crystals **47** before and after grinding under 365 nm UV light: (c) before grinding, (d) after grinding. Reproduced with permission [64]. Copyright 2014, The Royal Society of Chemistry (For interpretation of the references to color in this figure legend, the reader is referred to the web version of this article.).

also attributed to either CTA phase transition or CTC phase transition. Meanwhile, the MCL mechanisms of several binuclear gold(I) complexes are relevant with chemical reactions or are still unknown. In the following portion, a series of binuclear gold(I) complexes with or without AIE effect in response to mechanical stimulation will be introduced.

3.1. Binuclear MCL Au(I) complexes without AIE effect

3.1.1. The MCL phenomena resulting from CTA phase transition

Deák and coworkers reported a series of binuclear three-coordinate $[Au_2(xantphos)_2](X)_2$ ($X = NO_3$, CF_3SO_3, SCN, BF_4) and $[Au_2(nixantphos)_2](NO_3)_2$ (Fig. 21). As shown in Fig. 22, upon grinding, blue light-emitting crystalline **47** was converted into red luminescent powder with a large red-shift of 200 nm in emission [64]. Moreover, the initial blue emission could be recovered upon fuming the ground red light-emitting powder with dichloromethane vapor. PXRD experimental results confirmed that this observed reversible MCL phenomena were resulted from the mutual transformation between crystalline and amorphous states. The MCL behavior of gold(I) complex **48** was also checked, and

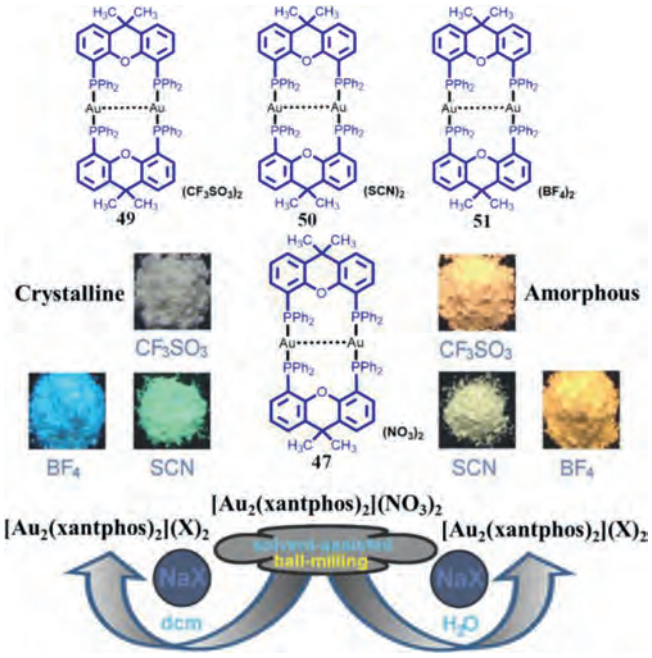

Fig. 23. Molecular structures of complexes **49–51** and photoluminescence images under 365 nm UV light of crystalline and amorphous **49–51** obtained from solvent-assisted ball-milling. Reproduced with permission [66]. Copyright 2014, The Royal Society of Chemistry.

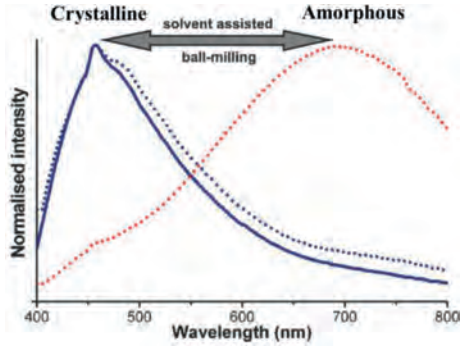

Fig. 24. Luminescence spectra of crystalline helicate **51**, amorphous helicate **51** obtained from crystalline helicate **51** *via* a water-assisted ball-milling, and crystalline helicate **51** obtained from amorphous helicate **51** *via* a dichloromethane-assisted ball-milling. Reproduced with permission [66]. Copyright 2014, The Royal Society of Chemistry.

the solid-state luminescent color of **48** could be switched effectively between ochre and dark red, which was attributed to the reversible transformation of crystalline and amorphous phases [65]. In 2014, Deák *et al.* prepared crystalline and amorphous dinuclear gold(I) helicates **49–51** with different anions *via* a high-efficiency solvent-assisted mechanochemical method [66]. Interestingly, the solid-state luminescence of crystalline **49–51** were different from their respective amorphous forms (Fig. 23). The crystalline helicates **49** and **51** were amorphized upon mechanical milling in the presence of water, and thus helicates **49** and **51** showed MCL features, while the helicate **50** still retained its crystalline nature even after mechanical milling for one hour. As can be seen in Fig. 24, helicate **51** exhibited a reversible MCL property with a high contrast between blue and orange-red colours, and the maximum emission wavelength exhibited a large reversible shift of 235 nm *via* the solvent-assisted ball-milling method.

Wolf *et al.* synthesized a binuclear gold(I) complex based on a terthienyl diphosphine ligand [67]. This gold(I) complex **52** was

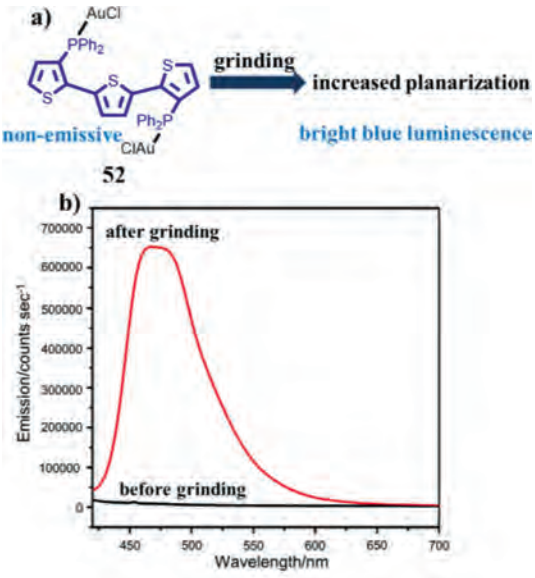

Fig. 25. (a) Molecular structure of complex **52** and the MCL schematic diagram of **52**. (b) Emission spectra of **52** before and after grinding. Reproduced with permission [67]. Copyright 2009, The Royal Society of Chemistry.

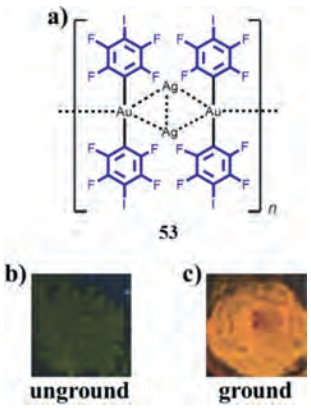

Fig. 26. (a) Molecular structure of complex **53**. Photoluminescence images under 365 nm UV light of before grinding (b) and after grinding (c). Reproduced with permission [68]. Copyright 2010, American Chemical Society (For interpretation of the references to color in this figure, the reader is referred to the web version of this article.).

non-emissive in the crystalline state, and an intense blue luminescence was observed when the initial sample was ground (Fig. 25), which was ascribed to the amorphization of as-prepared microcrystalline sample **52**. Meanwhile, the mechanically triggering blue emission was associated with increased planarization of a conjugated terthienyl ligand.

López-de-Luzuriaga *et al.* reported a yellow light-emitting $[Au_2Ag_2(4\text{-}C_6F_4I)_4]_n$ (**53**) (Fig. 26a) [68], and its emissive spectrum displayed an emission maximum at 577 nm. The initial yellow luminescence (Fig. 26b) could be switched to an intense orange luminescence (Fig. 26c) with a λ_{max} at 617 nm by grinding, and this observed MCL behavior of **53** was related with partial amorphization of crystalline sample **53**.

In 2015, Deák *et al.* reported five MCL $[Au_2(nixantphos)_2](X)_2$ ($X = NO_3$, **48**; CF_3COO, **54**; CF_3SO_3, **55**; $[Au(CN)_2]$, **56**; BF_4, **57**) (Fig. 27) [65]. Crystals **54** displayed switchable MCL quenching feature, and complex **55** displayed reversible MCL phenomenon involving the interconversion of yellow luminescence and red luminescence (Fig. 28). As shown in Fig. 29, crystals **56** exhibited MCL property accompanied with emission color changes from orange to red, and this MCL process was reversible. Complex **57** also exhibited reversible MCL switching between orange and dark red. The MCL phenomena of **48** and **54–57** were resulted from the CTA phase transition. In addition, variations in the N-H•••X hydrogen-bonding interactions between the $[Au_2(nixantphos)_2]^{2+}$

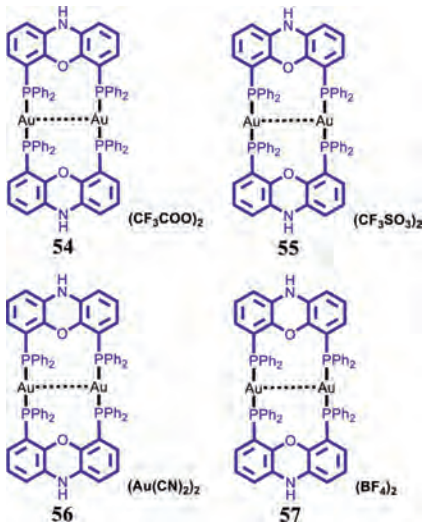

Fig. 27. Molecular structures of complexes **54–57**.

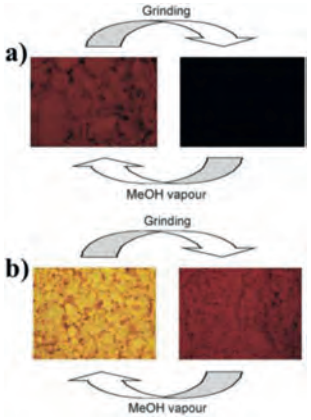

Fig. 28. (a) Photoluminescence images under 365 nm UV light of stimuli-responsive luminescence on–off switching of crystals **54**. (b) Photoluminescence images under 365 nm UV light of stimuli-responsive luminescence of **55**. Reproduced with permission [65]. Copyright 2015, Wiley-VCH (For interpretation of the references to color in this figure, the reader is referred to the web version of this article.).

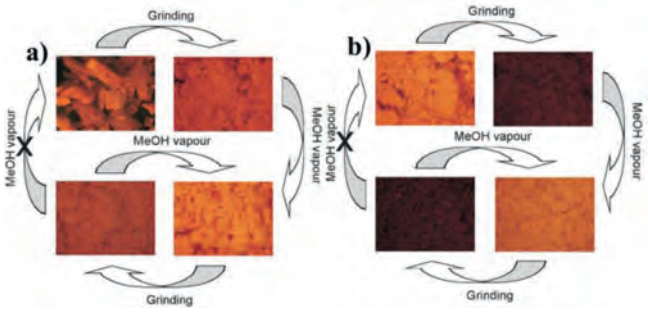

Fig. 29. (a) Photoluminescence images under 365 nm UV light of stimuli-responsive luminescence of crystals **56**. (b) Photoluminescence images under 365 nm UV light of stimuli-responsive luminescence of **57**. Reproduced with permission [65]. Copyright 2015, Wiley-VCH (For interpretation of the references to color in this figure, the reader is referred to the web version of this article.).

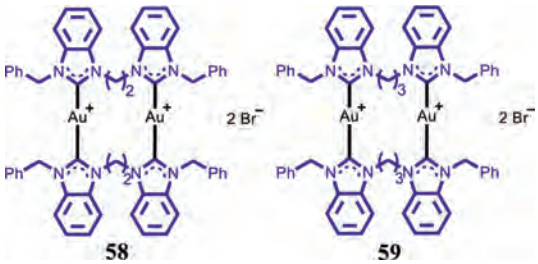

Fig. 30. Molecular structures of complexes **58** and **59**.

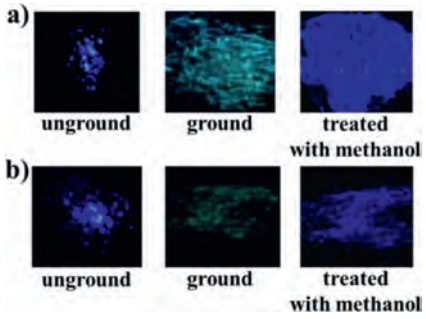

Fig. 31. (a) Photoluminescence images under 365 nm UV light of complex **58** in various solid states. (b) Photoluminescence images under 365 nm UV light of complex **59** in various solid states. Reproduced with permission [69]. Copyright 2016, American Chemical Society (For interpretation of the references to color in this figure, the reader is referred to the web version of this article.).

cations and X^- counteranions were also important factors for the formation of their MCL phenomena of **48** and **54–57**.

Penney *et al.* reported two reversible MCL dinuclear *N*-heterocyclic carbene gold(I) complexes **58** and **59** (Fig. 30) [69], which contained the bidentate benzimidazol-2-ylidene scaffold with alkyl spacers of different length. As presented in Fig. 31, the as-prepared solids **58** and **59** exhibited blue emission, which quickly changed into green luminescence upon grinding, and the mechanically induced solid-state green luminescence of **58** and **59** were reversed by exposure of the ground solids **58** and **59** to methanol or ethanol vapor. The observed MCL phenomena resulted from amorphization. Meanwhile, there may be a close relationship between bromide coordination and aurophilic interaction, and thus alterations in bromide coordination caused the corresponding changes in intramolecular aurophilic interactions, which possibly triggered mechano-responsive luminescence behaviors of **58** and **59**.

Liu *et al.* prepared a complex double salt $[Au(NHC)_2][Au(C{\equiv}N)_2]$ (NHC is referring to 1,3-dimethylimidazo[4,5-*b*]pyrazin-2-ylidene) by the method of co-precipitation of $[Au(NHC)_2]Cl$ and $K[Au(C{\equiv}N)_2]$ [70], which generated two distinct polymorphic crystals **60A** and **60B** that exhibited cyan and green luminescence, respectively. As shown in Fig. 32, for polymorph **60B**, upon small mechanical stimulus, the orange luminescent spots were noticed in where the mechanical force applied, and an orange light-emitting amorphous powder **60C** was observed by thoroughly grinding the crystals of polymorph **60B**. Similarly, cyan-emitting polymorph **60A** was also converted to orange luminescent powder **60C**. Interestingly, upon treatment of **60C** prepared by grinding the polymorph **60B** with CH_3OH solvent, the luminescent color of powder was restored to green, while the initial cyan luminescence could not be obtained upon treatment of **60C** prepared by grinding the polymorph **60A** with CH_3OH solvent, and the green luminescence of **60B** was seen.

Ito *et al.* reported reversible mechanochromic luminescence of a binuclear gold(I) isocyanide complex **61** (Fig. 33) [71]. In 2013,

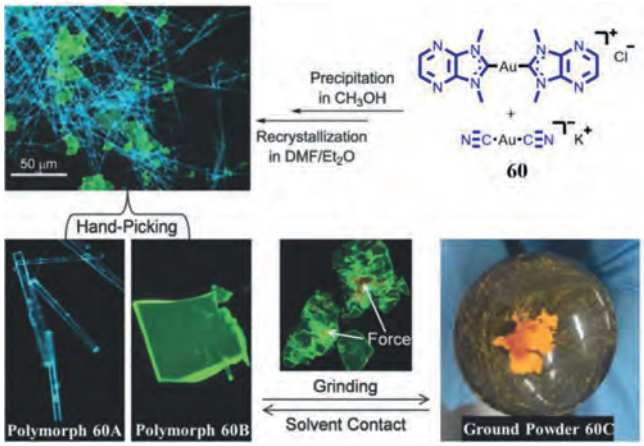

Fig. 32. Molecular structure of gold(I) double salt **60**, and the schematic diagrams of its polymorphism and mechanochromic luminescence. Reproduced with permission [70]. Copyright 2018, The Royal Society of Chemistry (For interpretation of the references to color in this figure, the reader is referred to the web version of this article.).

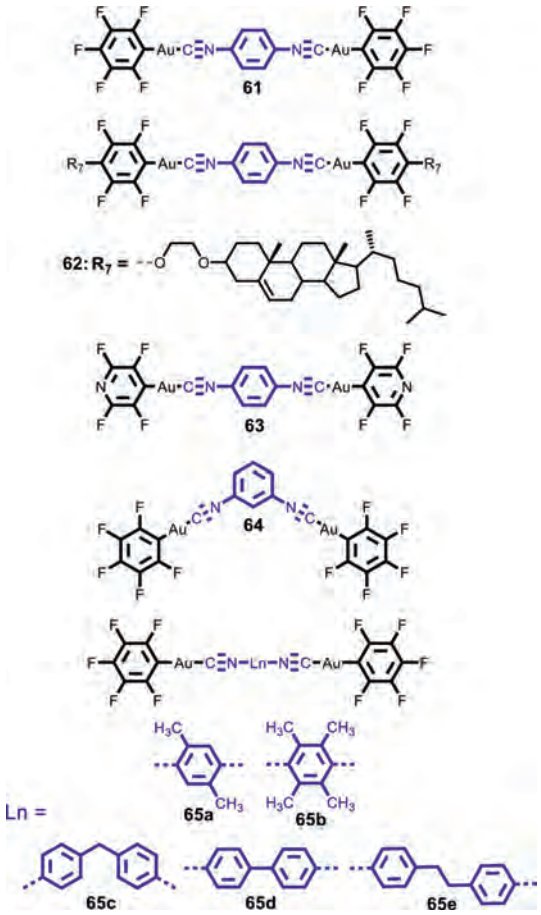

Fig. 33. Molecular structures of complexes **61–64** and complexes **65a–65e**.

Kawaguchi *et al.* prepared a MCL cholesterol-functionalized binuclear gold(I) complex **62**, and it formed two different microscopic structures through a cholesterol-aided self-organization process (Fig. 34) [72]. More specifically, self-organized semicrystalline fiber and noncrystalline globule were obtained by the method of vapor-diffusion of a poor solvent (acetone or methanol) into a dichloromethane solution containing complex **62**. Notably, the blue-emitting semicrystalline fibrous precipitates displayed MCL

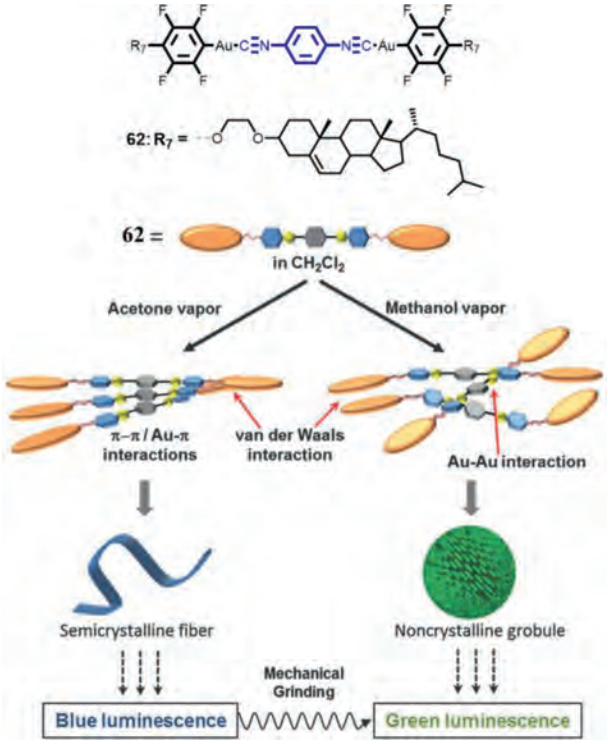

Fig. 34. Schematic diagram of solvent-assisted self-organization of **62** into two different microscopic structures. Reproduced with permission [72]. Copyright 2013, The Royal Society of Chemistry (For interpretation of the references to color in this figure, the reader is referred to the web version of this article.).

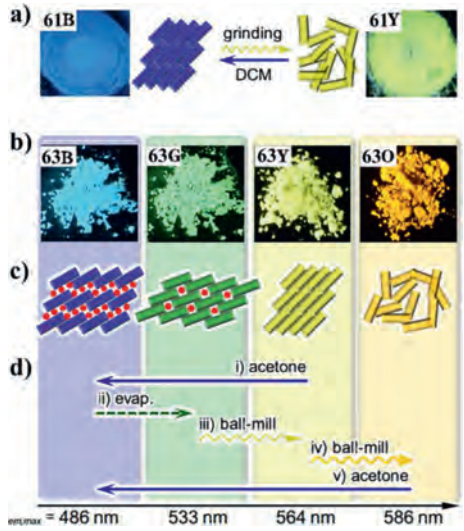

Fig. 35. (a) Photographs of complex **61** in various solid states under 365 nm UV light, and schematic diagram of the mechanism of its reversible MCL phenomenon. (b) Photographs of four different solid structures formed by complex **63** under 365 nm UV light. (c) Schematic diagram of molecular arrangements of four different solid structures formed by complex **63**. (d) Specific procedures for the interconversion of various emission colors of complex **63**. Reproduced with permission [73]. Copyright 2015, The Royal Society of Chemistry (For interpretation of the references to color in this figure, the reader is referred to the web version of this article.).

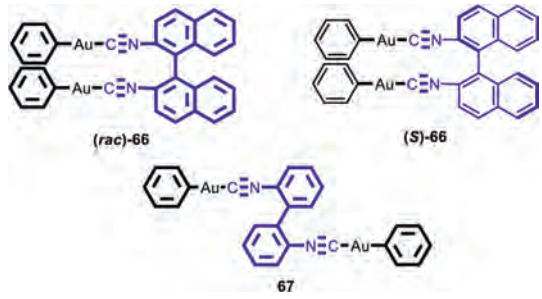

Fig. 36. Molecular structures of complexes (*rac*)–**66**, (*S*)–**66**, and **67**.

effect involving luminescent color changes of blue to green, which was similar with that of powder **62**. However, the green luminescent amorphous precipitates exhibited no MCL behavior. This work provided a deeper understanding of structural and MCL properties of a gold(I) complex. For complex **61**, its as-synthesized solid showed blue luminescence. Upon gentle grinding of sample **61**, a new emission band was observed, and a strong yellow luminescence was noticed under 365 nm UV light (Fig. 35a). The yellow light-emitting powder reverted back to the initial blue luminescence by the addition of several solvents involving ethyl acetate, diethyl ether and chloroform, or exposure to dichloromethane solvent vapor. Upon grinding, the crystalline state of the as-prepared sample **61** was converted into the amorphous state, which was confirmed by PXRD measurements. Yellow luminescence of ground sample **61** was possibly ascribed to the emergence of intermolecular aurophilic interactions after grinding.

Subsequently, in 2015, Seki *et al.* synthesized a multistimuli-responsive gold(I) complex **63** [73], which could afford four solid structures with four different luminescence (Fig. 35b). Upon different external stimuli, these various emission colors were interconvertible through structural changes (Figs. 35c and d). In particular, the green luminescence of **63** was changed into the orange luminescence by means of long ball-milling, and this mechanochromic process involved the CTA phase transition.

In 2018, Seki *et al.* prepared a *meta*-diisocyanide benzene-based binuclear gold(I) complex **64** [74], and this complex could form **64a–64g** with different crystal structures and various luminescent colors through effective crystallization procedures. All of the resulting solid-state structures of complex **64** showed clear MCL characteristics based on CTA phase transitions.

Liang *et al.* reported five binuclear gold(I) complexes **65a–65e** with different diisocyano bridges [75]. The five complexes displayed various mechanical-force-responsive behaviors. Complexes **65a–65c** with either methylsubstituted phenyl bridges or a diphenylmethane bridge exhibited MCL phenomena resulting from CTA phase transitions, while complexes **65d** and **65e** showed no MCL properties.

Seki *et al.* prepared two types of crystals with racemic or homochiral form from a gold(I) isocyanide complex possessing a binaphthyl unit (Fig. 36), and crystals of (*rac*)–**66** and (*S*)–**66** displayed different luminescence [76]. Upon mechanical grinding, their luminescence was converted into the similar emission colors due to CTA phase changes. In the same year, Seki and Ito *et al.* described an aryl gold isocyanide complex **67** with a biphenyl moiety [77]. Interestingly, the authors obtained **11** types of **67**/solvent samples possessing various emission properties *via* the addition of a variety of solvents, and thus **67** may be applied as a detector for different volatile organic compounds. Furthermore, single crystals of all these **67**/solvent samples and solvent-free **67**/none were successfully prepared (Fig. 37b). The 11 types of **67**/solvent samples showed distinct crystalline structures, and the crystalline phases and amorphous phases of these **67**/solvent samples could be interconverted by alternatingly applying mechanical grinding and solvent fuming (Fig. 37a).

3.1.2. The MCL phenomenon resulting from CTC phase transition

Tzeng and Chao obtained a dinuclear complex **68•2** CH_3CN [78], and the molecular structure of **68** is shown in Fig. 38a. The

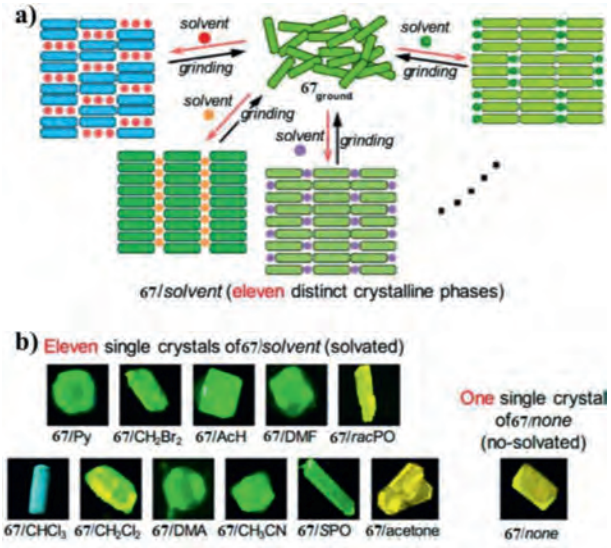

Fig. 37. (a) Schematic diagram of molecular arrangements of complex **67** caused by mechanical grinding and solvent addition. (b) Photographs of various single crystals of **67** under UV irradiation. Reproduced with permission [77]. Copyright 2016, American Chemical Society.

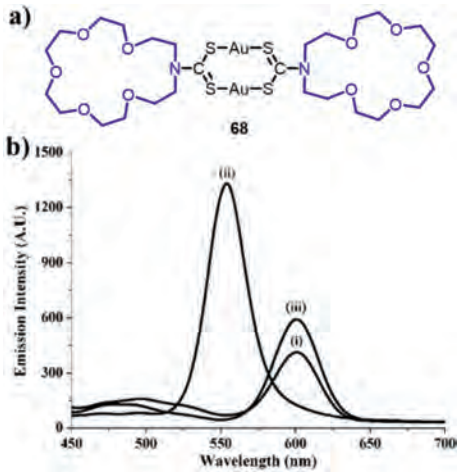

Fig. 38. (a) Molecular structure of complex **68**. (b) Photoluminescence spectra (excitation wavelength: 380 nm) of **68•2** CH_3CN in various states: (i) the as-prepared samples, (ii) the dry powder samples, (iii) the dry powder samples after grinding with CH_3CN. Reproduced with permission [78], Copyright 2015, Wiley-VCH.

as-prepared powder samples of **68•2** CH_3CN emitted red luminescence with an emission maximum at 602 nm (Fig. 38b, spectrum i), while the powder samples showed a new green emission band with a maximum at 553 nm upon drying under vacuum (Fig. 38b, spectrum ii). Moreover, the red luminescence could be recovered through further grinding with CH_3CN (Fig. 38b, spectrum iii). The variations of intermolecular aurophilic interactions in different conditions were responsible for these observed interesting phenomena.

3.1.3. The MCL phenomena resulting from CTC phase transition with a transient amorphous state

Ito and coworkers synthesized three MCL dinuclear Au(I) isocyanide complexes **69–71** with flexible side chains (Fig. 39). For complex **69**, its MCL characteristics involved an unusual CTC phase transition mediated by a transient amorphous phase (Fig. 40a) [79]. When the as-prepared blue light-emitting sample **69B** was ground with a spatula, a yellow light-emitting temporary **$69Y_m$** was formed, and the observed yellow luminescence was automatically converted to the initial blue luminescence within seconds. Notably, a green light-emitting **$69G_m$** was obtained by repeated grinding (Fig. 40b). Similarly, complexes **70** and **71** also exhibited rare MCL phenomena mediated by transient phases [80]. Moreover, the lifetimes of the transient amorphous phases of **69–71** were closely related with the structures of the terminal substituents of their side chains. Among them, complex **71** with the flexible hexyl units showed blue luminescence, and mechanical stimulation of blue light-emitting **71B** provided the transient amorphous **71Y** exhibiting yellow luminescence. Intriguingly, the yellow luminescence was immediately changed into the initial blue luminescence within 1 s.

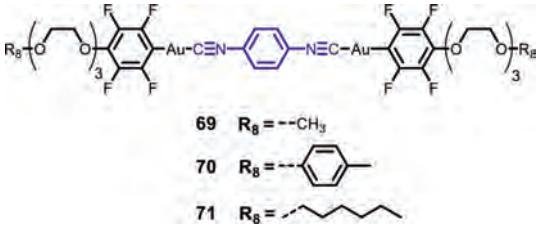

Fig. 39. Molecular structures of complexes **69–71**.

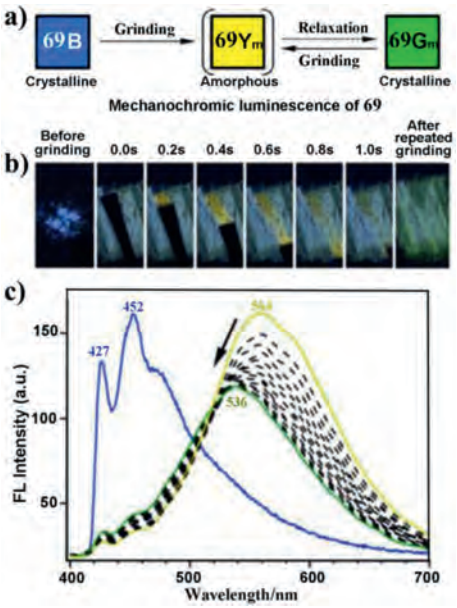

Fig. 40. (a) Schematic diagram of MCL behavior of complex **69**. (b) The photoluminescence photographs of **69** in various conditions. The left photograph shows the as-synthesized solid sample **69**. Photographs labeled from "0.0 s" to "1.0 s" show the transient **$69Y_m$** after grinding. The right photograph shows the **$69G_m$** formed by repeated grinding. (c) Blue line: emission spectrum of **69** before grinding. Progression of yellow to green lines: time-dependent emission spectra measured at 0.2 s intervals of **69** after grinding. Reproduced with permission [79]. Copyright 2016, American Chemical Society (For interpretation of the references to color in this figure legend, the reader is referred to the web version of this article.).

3.1.4. The MCL phenomena resulting from chemical reactions

Eisenberg and Lee reported two three-coordinate binuclear gold(I) thiouracilate complexes **72** and **73**, which were nonemissive [81]. However, blue luminescence for ground solid **72** and cyan luminescence for ground solid **73** were observed. The PXRD measurements indicated that no obvious phase changes for **72** and **73** could be seen before and after grinding. The MCL effect of **72** or **73** was triggered by molecular structure variation involving a solid-state chemical reaction. An infinite helical nonemissive **72** or **73** with weak intermolecular gold-gold interactions was rearranged into the corresponding aurophilically linked dimeric structure. Fur-

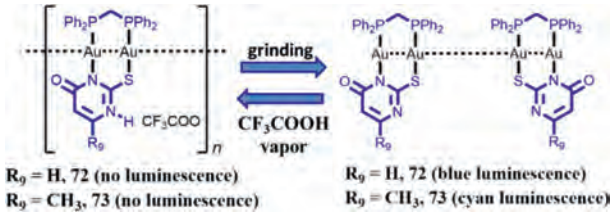

Fig. 41. Schematic diagram of MCL phenomena of binuclear complexes **72** and **73**.

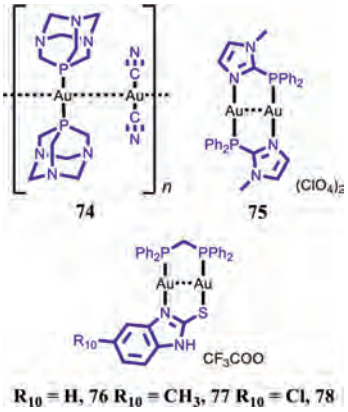

Fig. 42. Molecular structures of complexes **74–78**.

thermore, this process was reversible in the existence of CF_3COOH vapor (Fig. 41).

3.1.5. The MCL phenomena resulting from uncertain mechanisms

In 2002, Assefa *et al.* prepared a linearly coordinated gold(I) complex **74** (Fig. 42) simultaneously possessing thermochromic luminescence and MCL characteristics, which is the first example of MCL gold(I) complex [82]. Crystals **74** showed no luminescence, while a green luminescence was clearly observed after grinding. Catalano and Horner reported a three-coordinate binuclear gold(I) complex **75** (Fig. 42), and the complex exhibited strong intramolecular aurophilic interaction with short Au•••Au distance of 2.8261 Å [83]. Upon crushing, its orange-emitting crystals were converted to the blue luminescent powder. In 2008, Lee *et al.* reported three binuclear gold(I) complexes **76–78** (Fig. 42), and their three-coordinate gold(I) centres were closely connected through aurophilic interactions of 2.90607 Å for **76**, 2.8861 Å for **77**, 2.8807 Å for **78** [84]. Interestingly, upon gentle grinding, the blue luminescence of **76–78** changed into the luminescence with higher energies. As stated above, gold(I) complexes **74–78** displayed notable MCL behaviors. However, it is regrettable that the MCL mechanisms of **74–78** still have not been reported.

3.2. Binuclear AIE-active Au(I) complexes with MCL phenomena resulting from CTA phase transition

Liang *et al.* synthesized three diisocyano-based donor-acceptor (D-A) type gold(I) complexes **79a–79c** (Fig. 43), and these complexes showed remarkable AIE phenomena [85]. In addition, **79a–79c** also exhibited unusual "off-on" switchable MCL behaviors, which were driven by CTA morphological transition. Furthermore, the repeatabilities of their MCL phenomena were outstanding.

In 2015, Chen *et al.* reported a fluorene-based AIE-active dinuclear gold(I) isocyanide complex **80** [86]. The complex displayed strong yellow luminescence in the aggregation state. In the solid state, complex **80** emitted green luminescence, and its green luminescence was changed into yellow luminescence upon grinding

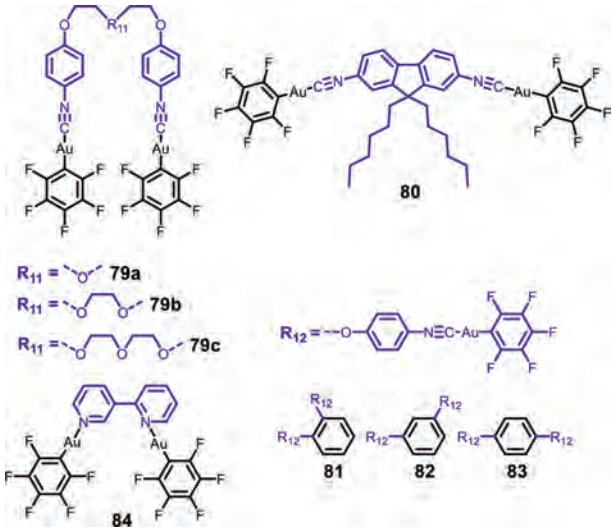

Fig. 43. Molecular structures of complexes **79a–79c** and **80–84**.

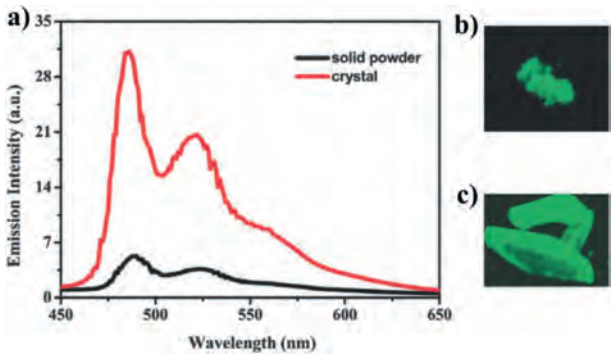

Fig. 44. (a) Emission spectra of solid powder and crystals of complex **80**. Photographic images of solid powder (b) and crystals (c) of complex **80** under 365 nm UV light. Reproduced with permission [86]. Copyright 2015, The Royal Society of Chemistry (For interpretation of the references to color in this figure, the reader is referred to the web version of this article.).

the powder sample of **80**. The observed mechanical force-induced yellow luminescence reverted back to the green emission after treatment with fuming dichloromethane vapor. On the other hand, luminogen **80** also showed crystallization-induced emission enhancement feature (Fig. 44). In the same year, Chen *et al.* reported three constitutional isomeric dinuclear gold(I) complexes **81–83** [87]. Although luminogens **81–83** exhibited similar AIE characteristics, the different mechano-responsive behaviors of **81–83** were noticed. For *ortho*-isomer **81**, it showed reversible MCL conversion between blue and green emission colors. For *meta*-isomer **82**, it showed switchable mechanical stimulation-induced luminescence enhancement behavior. As for *para*-isomer **83**, it displayed negligible MCL phenomenon. In 2018, Chen *et al.* described a bipyridine-based binuclear gold(I) complex **84** with AIE and self-assembly characteristics [88]. This complex also showed reversible phosphorescent mechanochromism, and its mechanochromic process involved the CTA phase transition.

4. Mechanochromic luminescence of multinuclear gold(I) complexes

To date, some MCL multinuclear gold(I) complexes have been discovered, and the MCL phenomena of these multinuclear gold(I) complexes are attributed to CTA phase transition. In the following

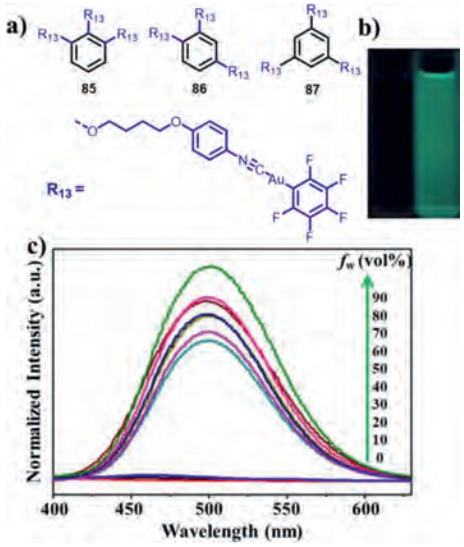

Fig. 45. (a) Molecular structures of complexes **85–87**. (b) Photographic images of **85** in pure DMF as well as 90% water fraction under 365 nm UV light. (c) Emission spectra of **85** in DMF-H_2O mixtures with various water fractions, excitation wavelength: 330 nm. Reproduced with permission [89]. Copyright 2015, Elsevier Ltd. (For interpretation of the references to color in this figure, the reader is referred to the web version of this article.).

portion, several multinuclear MCL gold(I) complexes with or without AIE effect will be introduced.

4.1. Trinuclear AIE-active Au(I) complexes with MCL phenomena resulting from CTA phase transition

Chen *et al.* synthesized three triisocyano-based constitutional isomers **85–87** containing trinuclear gold(I) units (Fig. 45a) [89], and these gold(I) complexes displayed similar AIE and mechanoresponsive luminescence behaviors. Taking complex **85** as a representative example, as presented in Figs. 45b and c, **85** was nearly nonemissive when its diluted DMF solution (1.0×10^{-5} mol/L) was photoexcited. In contrast, a strong green emission band appeared and the bright green luminescence was observed upon aggregation, indicating its typical AIE feature. Furthermore, upon grinding, luminogen **85** displayed "off-on" green luminescence, which was caused by CTA morphological transformation.

4.2. Six-nuclear non-AIE-active Au(I) complexes with MCL phenomena resulting from CTA phase transition

Walters *et al.* prepared three gold(I) complexes **88B–90B** with a boxlike skeleton, and their molecular structures were crystallographically characterized [90]. After mechanical grinding, blue light-emitting crystals containing the same cation $[Au_6(Triphos)_4Cl]^{5+}$ of **88B–90B** were converted into the corresponding amorphous green light-emitting solids possessing the bridged helicate cation $[\mu\text{-}Cl\{Au_3(Triphos)_2\}_2]^{5+}$ (Fig. 46). On the other hand, the authors confirmed that a triphosphine ligand exhibiting no luminescence could be applied to construct a luminescent container cation containing six gold(I) ions.

4.3. Octanuclear non-AIE-active Au(I) complex with MCL phenomenon resulting from CTA phase transition

In 2011, Koshevoy and Chou synthesized an octanuclear gold(I) cluster complex **91** containing alkynyl-diphosphine ligands (Fig. 47), and its crystals of **91** emitted red luminescence [91]. After fully grinding of the crystals, the emission band with a λ_{max}

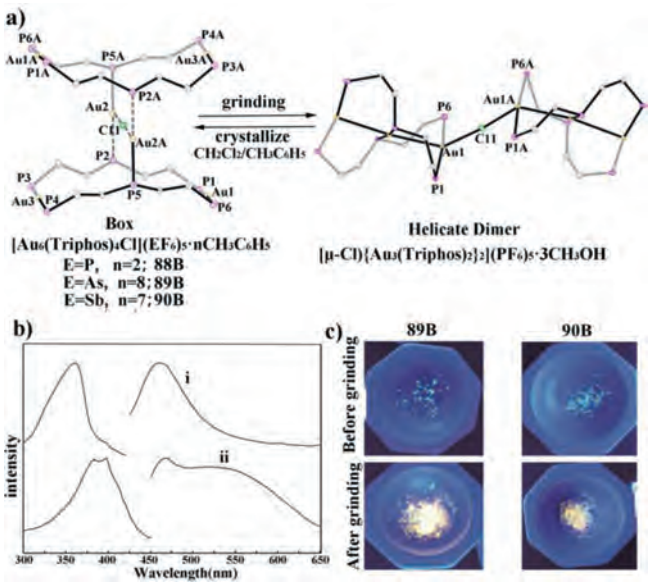

Fig. 46. (a) Schematic diagram of reversible mechanochromic phenomena of **88B–90B**. Triphos = bis(2-diphenylphosphinoethyl)phenylphosphine). The solvent molecules, phenyl rings, and five hexafluorophosphate, hexafluoroarsenate or hexafluoroantimonate anions are omitted. (b) Excitation (i, left) and emission (i, right) spectra at 22 °C of unground crystals of **90B**; Excitation (ii, left) and emission (ii, right) spectra at 22 °C of ground crystals of **90B** (c) Photographic images of unground **89B**, **90B** (top) and ground **89B**, **90B** (bottom) at 22 °C under UV irradiation. Reproduced with permission [90]. Copyright 2018, American Chemical Society (For interpretation of the references to color in this figure, the reader is referred to the web version of this article.).

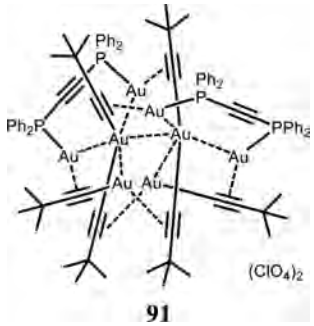

Fig. 47. Molecular structure of gold(I) cluster complex **91**.

at 730 nm almost completely disappeared, and a new yellowish-green-emitting emission band with a λ_{max} at 560 nm appeared. The emission band of ground crystals **91** was similar to that of **91** in CH_2Cl_2 solution. This MCL effect of **91** was ascribed to CTA phase transition. For crystals **91**, as demonstrated by extended X-ray absorption fine structure (EXAFS) data, upon grinding, some Au-Au bond distances might become closer, which resulted in the increase of coordination number of Au-Au, and the amorphous structure with the loss of lattice energy after grinding might be similar to that of **91** in CH_2Cl_2 solution.

5. Summary and outlook

In this review, an overview of the research progress on MCL gold(I) complexes has been presented. The reported MCL gold(I) systems involve mononuclear, binuclear, and multinuclear gold(I) complexes. Furthermore, some MCL gold(I)-containing complexes have been proved to be able to display typical AIE characteristics. Single crystal X-ray diffraction and PXRD measurements provide significant information for sources of the observed MCL phenom-

ena of these gold(I) complexes. On the whole, their MCL mechanisms are resulted from either CTA phase transition or CTC phase transition. Meanwhile, the mechanoluminochromic mechanisms of several gold(I) complexes are still unknown. Nevertheless, in our opinion, it is speculated that the MCL phenomena of these gold(I) complexes are possibly attributed to CTA phase transition. During their MCL processes, alterations in multiple intermolecular weak interactions (C-H•••π, π•••π, C-H•••O, C-H•••N, C-H•••F, C-H•••S, *etc*.) and intermolecular aurophilic interactions play important roles in promoting effective mechanical force-responsive luminescent phenomena. Although a series of MCL gold(I)-based luminophors have been discovered, the number of high-contrast MCL gold(I) complexes, especially the AIE-active high-contrast mechanically responsive gold(I) complexes, is still inadequate because of the lacking of effective guidelines for preparing the corresponding smart molecules. AIE-active luminophors can exhibit strong luminescence upon aggregation, which is beneficial for achieving high-contrast mechanoluminochromic phenomena. Therefore, AIE-active MCL gold(I) complexes may become an important source of high-performance gold(I)-containing mechanoresponsive luminescent materials in the future. Further systematic investigation on structures-properties relationships of MCL gold(I) complexes is still a meaningful and challenging subject. Meanwhile, the related research of the potential applications of MCL gold(I) complexes in the fields of sensors, anti-counterfeiting and luminescent switches remains to be explored. We enthusiastically expect that this review can provide a valuable reference for scientists in this fascinating area of research.

Declaration of competing interest

The authors declare no conflict of interest.

Acknowledgments

The authors acknowledge financial support from the National Natural Science Foundation of China (Nos. 22061018, 21702079 and 21772054), and the startup funding from South-Central University for Nationalities (No. YZZ19005).

References

[1] A.C. Grimsdale, K.L. Chan, R.E. Martin, P.G. Jokisz, A.B. Holmes, Chem. Rev. 109 (2009) 897–1091.
[2] M.M. Islam, Z. Hu, Q. Wang, C. Redshaw, X. Feng, Mater. Chem. Front. 3 (2019) 762–781.
[3] E. Cariati, E. Lucenti, C. Botta, et al., Coord. Chem. Rev. 306 (2016) 566–614.
[4] S. Kang, J.S. Huh, J.J. Kim, J. Park, J. Mater. Chem. C 8 (2020) 11168–11176.
[5] Z. Zhang, Y. Li, X. Wu, W. Chu, S. Yin, J. Mater. Chem. C 8 (2020) 11239–11251.
[6] T. Sudyoadsuk, P. Chasing, C. Chaiwai, et al., J. Mater. Chem. C 8 (2020) 10464–10473.
[7] C.L. Wong, M. Ng, E.Y.H. Hong, et al., J. Am. Chem. Soc. 142 (2020) 12193–12206.
[8] S. Sonalin, A. Mishra, A.K. Sahu, et al., J. Phys. Chem. C 124 (2020) 13053–13062.
[9] H.T. Mao, G.F. Li, G.G. Shan, X.L. Wang, Z.M. Su, Coord. Chem. Rev. 413 (2020) 213283.
[10] L. Tu, Y. Xu, Q. Ouyang, X. Li, Y. Sun, Chin. Chem. Lett. 30 (2019) 1731–1737.
[11] Q. Lin, Z. Li, Q. Yuan, Chin. Chem. Lett. 30 (2019) 1547–1556.
[12] D. Li, W. Chen, S.H. Liu, X. Chen, J. Yin, Chin. Chem. Lett. 31 (2020) 2891–2896.
[13] F. Ciardelli, G. Ruggeri, A. Pucci, Chem. Soc. Rev. 42 (2013) 857–870.
[14] P. Xue, J. Ding, P. Wang, R. Lu, J. Mater. Chem. C 4 (2016) 6688–6706.
[15] Z. Yang, Z. Chi, Z. Mao, et al., Mater. Chem. Front. 2 (2018) 861–890.
[16] J. Zhao, Z. Chi, Z. Yang, et al., Mater. Chem. Front. 2 (2018) 1595–1608.
[17] S. Xue, X. Qiu, Q. Sun, W. Yang, J. Mater. Chem. C 4 (2016) 1568–1578.
[18] Z. Chen, J.H. Tang, W. Chen, et al., Organometallics 38 (2019) 4244–4249.
[19] Y. Yin, Z. Chen, R.H. Li, et al., Inorg. Chem. (2021), doi:10.1021/acs.inorgchem.1c00233.
[20] Z. He, W. Li, G. Chen, Y. Zhang, W.Z. Yuan, Chin. Chem. Lett. 30 (2019) 933–936.
[21] B. Lu, S. Liu, D. Yan, Chin. Chem. Lett. 30 (2019) 1908–1922.
[22] N. Mirzadeh, S.H. Privér, A.J. Blake, H. Schmidbaur, S.K. Bhargava, Chem. Rev. 120 (2020) 7551–7591.
[23] Z. Chen, D. Wu, X. Han, et al., Chem. Commun. 50 (2014) 11033–11035.
[24] H. Schmidbaur, H.G. Raubenheimer, Angew. Chem. Int. Ed. 59 (2020) 14748–14771.
[25] Y. Dong, F. Zhu, Z. Chen, J. Yin, S.H. Liu, Mater. Chem. Front. 3 (2019) 1866–1871.
[26] H. Schmidbaur, A. Schier, Chem. Soc. Rev. 41 (2012) 370–412.
[27] X.Y. Wang, Y.X. Hu, X.F. Yang, et al., Org. Lett. 21 (2019) 9945–9949.
[28] G.J. Hutchings, M. Brust, H. Schmidbaur, Chem. Soc. Rev. 37 (2008) 1759–1765.
[29] A. Pinto, N. Svahn, J.C. Lima, L. Rodríguez, Dalton Trans. 46 (2017) 11125–11139.
[30] E.R.T. Tiekink, Coord. Chem. Rev. 275 (2014) 130–153.
[31] S. Sculfort, P. Braunstein, Chem. Soc. Rev. 40 (2011) 2741–2760.
[32] X.S. Xiao, C. Zou, X. Guan, et al., Chem. Commun. 52 (2016) 4983–4986.
[33] J.G. Yang, K. Li, J. Wang, et al., Angew. Chem. Int. Ed. 59 (2020) 6915–6922.
[34] Z. Luo, X. Yuan, Y. Yu, et al., J. Am. Chem. Soc. 134 (2012) 16662–16670.
[35] J. Liang, Z. Chen, J. Yin, G.A. Yu, S.H. Liu, Chem. Commun. 49 (2013) 3567–3569.
[36] A.L. Balch, Angew. Chem. Int. Ed. 48 (2009) 2641–2644.
[37] M. Osawa, I. Kawata, S. Igawa, et al., Chem. Eur. J. 16 (2010) 12114–12126.
[38] P. Baranyai, G. Marsi, C. Jobbágy, et al., Dalton Trans 44 (2015) 13455–13459.
[39] T. Seki, N. Tokodai, S. Omagari, et al., J. Am. Chem. Soc. 139 (2017) 6514–6517.
[40] T. Seki, K. Kobayashi, T. Mashimo, H. Ito, Chem. Commun. 54 (2018) 11136–11139.
[41] Y.B. Dong, Z. Chen, L. Yang, et al., Dyes Pigm. 150 (2018) 315–322.
[42] Z. Chen, Y. Yin, S. Pu, S.H. Liu, Dyes Pigm. 184 (2021) 108814.
[43] Z. Chen, G. Liu, R. Wang, S. Pu, RSC Adv. 7 (2017) 15112–15115.
[44] Z. Chen, G. Liu, S. Pu, S.H. Liu, Dyes Pigm. 159 (2018) 499–505.
[45] M.J. Wang, Z.Y. Wang, P. Luo, et al., Cryst. Growth Des. 19 (2019) 538–542.
[46] V. Conejo-Rodríguez, M.N. Peñas-Defrutos, P. Espinet, Dalton Trans. 48 (2019) 10412–10416.
[47] H. Ito, M. Muromoto, S. Kurenuma, et al., Nat. Commun. 4 (2013) 2009–2013.
[48] T. Seki, K. Sakurada, H. Ito, Angew. Chem. Int. Ed. 52 (2013) 12828–12832.
[49] T. Seki, K. Sakurada, H. Ito, Chem. Commun. 51 (2015) 13933–13936.
[50] T. Seki, K. Kobayashi, H. Ito, Chem. Commun. 53 (2017) 6700–6703.
[51] T. Seki, Y. Takamatsu, H. Ito, J. Am. Chem. Soc. 138 (2016) 6252–6260.
[52] K. Sakurada, T. Seki, H. Ito, CrystEngComm 18 (2016) 7217–7220.
[53] M. Jin, T. Seki, H. Ito, J. Am. Chem. Soc. 139 (2017) 7452–7455.
[54] M. Jin, T. Sumitani, H. Sato, T. Seki, H. Ito, J. Am. Chem. Soc. 140 (2018) 2875–2879.
[55] A. Sathyanarayana, S.Y. Nakamura, K. Hisano, et al., Sci. China Chem. 61 (2018) 957–965.
[56] X.Y. Wang, J. Zhang, J. Yin, S.H. Liu, Chem. Asian J. 14 (2019) 2903–2910.
[57] E.J. Fernández, J.M. López-de-Luzuriaga, M. Monge, et al., J. Am. Chem. Soc. 125 (2003) 2022–2023.
[58] A. Deák, T. Tunyogi, G. Pálinkás, J. Am. Chem. Soc. 131 (2009) 2815–2817.
[59] Z. Chen, L. Yang, Y. Hu, et al., RSC Adv. 5 (2015) 93757–93764.
[60] Z. Chen, Z. Li, F. Hu, et al., Dyes Pigm. 125 (2016) 169–178.
[61] Z. Chen, Y. Nie, S.H. Liu, RSC Adv. 6 (2016) 73933–73938.
[62] Z. Chen, G. Liu, S. Pu, S.H. Liu, Dyes Pigm. 143 (2017) 409–415.
[63] W.B. Li, W.J. Luo, K.X. Li, W.Z. Yuan, Y.M. Zhang, Chin. Chem. Lett. 28 (2017) 1300–1305.
[64] C. Jobbágy, M. Molnár, P. Baranyai, et al., CrystEngComm 16 (2014) 3192–3202.
[65] A. Deák, C. Jobbágy, G. Marsi, et al., Chem. Eur. J. 21 (2015) 11495–11508.
[66] C. Jobbágy, M. Molnár, P. Baranyai, A. Deák, Dalton Trans. 43 (2014) 11807–11810.
[67] A.M. Kuchison, M.O. Wolf, B.O. Patrick, Chem. Commun. (2009) 7387–7389.
[68] A. Laguna, T. Lasanta, J.M. López-de-Luzuriaga, et al., J. Am. Chem. Soc. 132 (2010) 456–457.
[69] A.A. Penney, V.V. Sizov, E.V. Grachova, et al., Inorg. Chem. 55 (2016) 4720–4732.
[70] Q. Liu, M. Xie, X. Chang, et al., Chem. Commun. 54 (2018) 12844–12847.
[71] H. Ito, T. Saito, N. Oshima, et al., J. Am. Chem. Soc. 130 (2008) 10044–10045.
[72] K. Kawaguchi, T. Seki, T. Karatsu, et al., Chem. Commun. 49 (2013) 11391–11393.
[73] T. Seki, T. Ozaki, T. Okura, et al., Chem. Sci. 6 (2015) 2187–2195.
[74] T. Seki, K. Ida, H. Ito, Mater. Chem. Front. 2 (2018) 1195–1200.
[75] J. Liang, F. Hu, X. Lv, et al., Dyes Pigm. 95 (2012) 485–490.
[76] M. Jin, T. Seki, H. Ito, Chem. Commun. 52 (2016) 8083–8086.
[77] T. Seki, M. Jin, H. Ito, Inorg. Chem. 55 (2016) 12309–12320.
[78] B.C. Tzeng, A. Chao, Chem. Eur. J. 21 (2015) 2083–2089.
[79] S. Yagai, T. Seki, H. Aonuma, et al., Chem. Mater. 28 (2016) 234–241.
[80] T. Seki, K. Kashiyama, S. Yagai, H. Ito, Chem. Lett. 46 (2017) 1415–1418.
[81] Y.A. Lee, R. Eisenberg, J. Am. Chem. Soc. 125 (2003) 7778–7779.
[82] Z. Assefa, M.A. Omary, B.G. McBurnett, et al., Inorg. Chem. 41 (2002) 6274–6280.
[83] V.J. Catalano, S.J. Horner, Inorg. Chem. 42 (2003) 8430–8438.
[84] J. Schneider, Y.A. Lee, J. Pérez, et al., Inorg. Chem. 47 (2008) 957–968.
[85] J. Liang, Z. Chen, L. Xu, et al., J. Mater. Chem. C 2 (2014) 2243–2250.
[86] Z. Chen, J. Zhang, M. Song, et al., Chem. Commun. 51 (2015) 326–329.
[87] Z. Chen, Z. Li, L. Yang, et al., Dyes Pigm. 121 (2015) 170–177.
[88] Z. Chen, G. Liu, S. Pu, S.H. Liu, Dyes Pigm. 152 (2018) 54–59.
[89] Z. Chen, P.S. Huang, Z. Li, et al., Inorgan. Chim. Acta 432 (2015) 192–197.
[90] D.T. Walters, R.B. Aghakhanpour, X.B. Powers, et al., J. Am. Chem. Soc. 140 (2018) 7533–7542.
[91] I.O. Koshevoy, C.L. Lin, A.J. Karttunen, et al., Chem. Commun. 47 (2011) 5533–5535.